

1 This is a non-peer reviewed preprint submitted to EarthArXiv. This preprint has been submitted
2 for peer review at American Journal of Science:

3

4 **Regional trends and petrologic factors inhibit global interpretations of zircon**
5 **trace element compositions**

6

7 Nick M W Roberts^{1*}, Christopher J Spencer², Stephen Puetz³, C. Brenhin Keller⁴, Simon Tapster¹

8

9 ¹Geochronology and Tracers Facility, British Geological Survey, Nottingham, NG12 5GG, UK

10 ²Department of Geological Sciences and Geological Engineering, Queen's University, Kingston,
11 Ontario, Canada

12 ³475 Atkinson Dr, Suite 704, Honolulu, HI 96814, USA

13 ⁴Department of Earth Sciences, Dartmouth College, Hanover, New Hampshire, USA

14

15 *Corresponding author (email: nirob@bgs.ac.uk)

16

17 **Regional trends and petrologic factors inhibit global interpretations of zircon**
18 **trace element compositions**

19

20 Nick M W Roberts^{1*}, Christopher J Spencer², Stephen Puetz³, C. Brenhin Keller⁴, Simon Tapster¹

21

22 ¹Geochronology and Tracers Facility, British Geological Survey, Nottingham, NG12 5GG, UK

23 ²Department of Geological Sciences and Geological Engineering, Queen's University, Kingston,
24 Ontario, Canada

25 ³475 Atkinson Dr, Suite 704, Honolulu, HI 96814, USA

26 ⁴Department of Earth Sciences, Dartmouth College, Hanover, New Hampshire, USA

27

28 *Corresponding author (email: nirob@bgs.ac.uk)

29

30 NR: 0000-0001-8272-5432

31 CS: 0000-0003-4264-3701

32 SP: 0000-0002-8842-9754

33 CBK: 0000-0001-7400-9428

34 ST: 0000-0001-9049-0485

35

36 **Keywords**

37 Detrital zircon; trace elements; secular change; Eu anomaly; crustal thickness;

38

39

40 **Abstract**

41 The trace element composition of zircon reveals information about the melt that they are derived
42 from, as such, detrital zircon trace element compositions can be used to interrogate melt
43 compositions, and thus the evolution of the continental crust in time and space. Here, we present
44 a global database of detrital zircon compositions and use it to test whether average global trends
45 for five common petrogenetic proxies truly represent secular changes in continental evolution.
46 We demonstrate that the secular trend is broadly comparable across continental regions for Ti-in-
47 zircon temperatures, but for other trace element ratios interrogated, secular trends are highly
48 variable between continental regions. Because trace element ratios result from multiple petrologic
49 variables, we argue that these petrogenetic proxies can be overinterpreted if projected to global
50 geologic processes. In particular, we caution against the interpretation of crustal thickness from
51 trace elements in zircon, and we argue that our results negate current hypotheses concerning
52 secular changes in crustal thickness.

53

54 **1. Introduction**

55 Due to its physical and chemical resilience, zircon remains the most popular mineral for studying
56 the long-term evolution of Earth's continental crust. Detrital zircon datasets have broad spatial
57 and temporal coverage of the continents, and beyond the use of sediment provenance, are
58 commonly used to understand secular changes in magmatic and metamorphic processes (Roberts
59 and Spencer, 2015). In the last few years, there has been a significant rise in the use of zircon
60 trace element compositions to track secular change in continental evolution on both regional
61 (Brudner et al., 2022; Liu et al., 2022; Wu et al., 2023) and global scales (McKenzie et al., 2018;
62 Balica et al., 2020; Tang et al., 2021b; Verdel et al., 2021; Paulsen et al., 2022). This rise is
63 driven by the use of trace element proxies as petrogenetic indicators, for example, Ti as a
64 function of temperature (Watson) and Eu/Eu* as a proxy for crustal thickness (Tang et al., 2021).

65

66 To date, global detrital zircon trace element compilations have not been exhaustive, generally
67 comprising <10000 records, and biased towards certain regions (e.g. McKenzie et al., 2018;
68 Balica et al., 2020; Paulsen et al., 2021; Verdel et al., 2021; Tang et al., 2021b; Triantafyllou et
69 al., 2022). This begs the important question, to what extent are these datasets representative of
70 global processes? For Hf isotopes, Sundell and Macdonald (2022) conducted a study using the
71 Puetz et al. (2021) database (n = 165,111) into regional variance and demonstrated that global

72 trends reflect the evolution of specific orogens, which do not necessarily reflect contemporaneous
73 secular evolution of global processes. Furthermore, the direct use of most petrogenetic proxies is
74 often heavily caveated and/or shown to be problematic (e.g. Triantafyllou et al., 2022), but these
75 issues tend not to deter their use (e.g. Wu et al., 2023).

76

77 Here, we present an updated literature compilation of trace element compositions of detrital
78 zircon, comprising ~43000 filtered analyses (n = ~77000 unfiltered). The aim of this contribution
79 is threefold: 1) present an updated comprehensive global compilation that is open access and
80 comprises thorough metadata records; 2) test global trends in common petrogenetic proxies to
81 demonstrate the potential effects of regional bias; and 3) comment on the robustness of the most
82 common petrogenetic proxies in light of our findings and incorporating known issues and
83 caveats.

84

85 **2. Methods and data**

86 Trace element compositions of zircon were collated from 112 literature sources, comprising 562
87 individual samples, and 77127 individual records. We aimed to provide a comprehensive
88 coverage of the current literature; in general, most omitted publications are scant in metadata or
89 contain very few individual records. Correlative age data were collected for a subset of data,
90 generally where they were provided in the same format and/or in the same data tables. Compiled
91 metadata include location information: continent, country, location, and GPS coordinates in a
92 common UTM format. The locations are taken from the original sources, and where not provided,
93 estimated from published map figures. The database is provided in full at

94 <https://figshare.com/s/89d01010d6a7ba4c9592>

95

96

97 For our analysis of global trends, we have filtered the data for discordance, inclusions, and
98 anomalous values, and provided a 'best age' for each record. Trends of elemental concentration
99 or element ratio with age are shown as means, binned at 100 Myr intervals, and calculated using a
100 weighted bootstrap resampling method following Keller and Schoene (2012). This approach
101 helps alleviate sampling bias by assigning each sample a resampling probability that is inversely
102 correlated to spatial and temporal sample density (Keller and Schoene, 2012). Details of filtering,

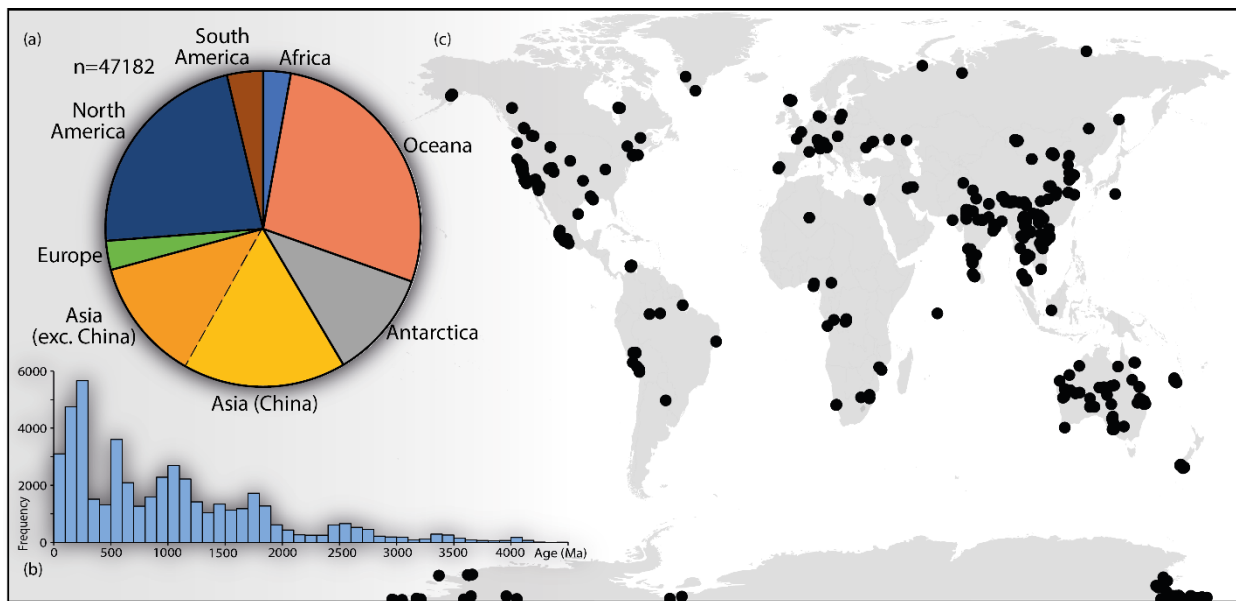
103 choice of age, and plotting are described in the supplementary text. Additional figures comprising
104 alternative methods for plotting secular trends are also included in the supplementary files.

105

106 3. Results

107 Our filtered database comprises 47182 records and covers all continents; however, there is
108 sampling bias towards certain regions, with Africa and South America having disproportionately
109 low abundance (Figure 1a). The records span Earth's history with increasing density through time
110 (Figure 1b). In Figure 1c it can be seen that the data have broad global coverage, but with
111 significant continental areas still missing any records. Any hypotheses regarding global processes
112 should be aware of these discrepancies in global coverage, even if attempts are made to account
113 for regional bias with statistical methods (e.g. Keller and Schoene, 2012). Noting the still existent
114 regional bias in the database, it is still somewhat more extensive than those used previously (e.g.
115 Balica et al., 2020; Tang et al., 2021b; Verdel et al., 2021; Deering et al., 2022).

116



117

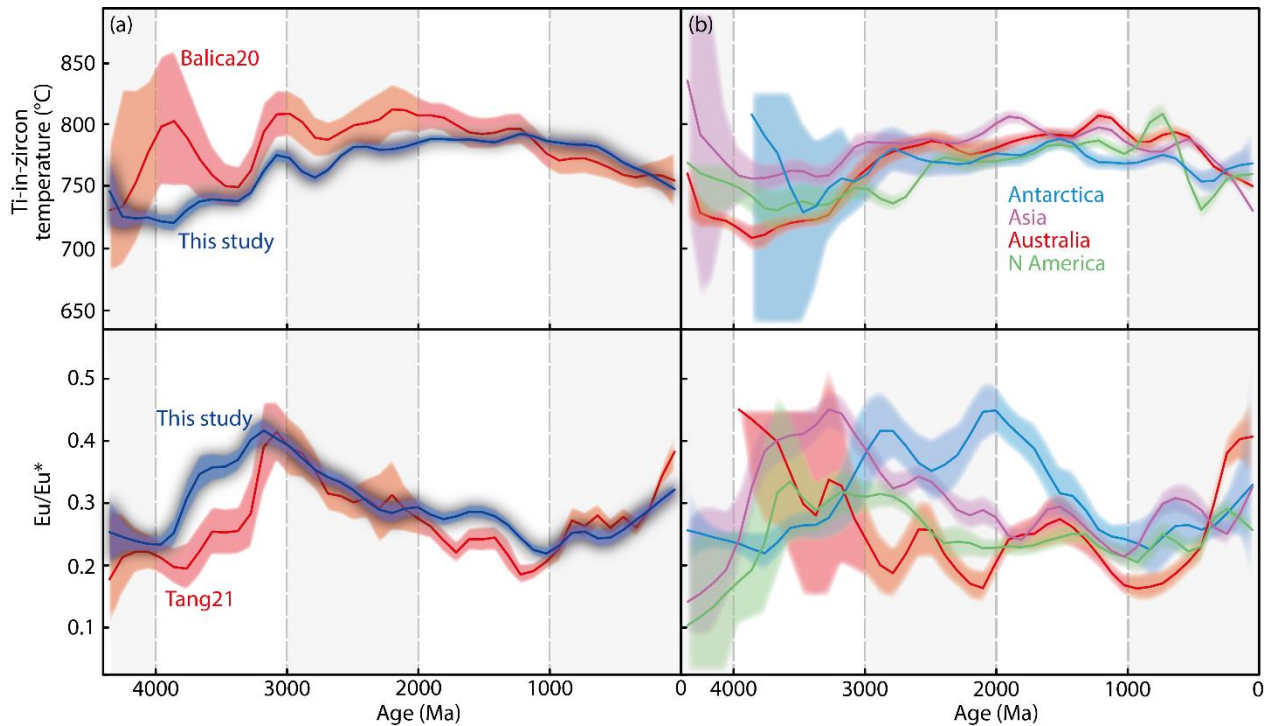
118 **Figure 1 (a)** Pie chart showing the density of detrital zircon per continent (filtered dataset). **(b)**
119 Histogram (100 Myr binwidth) of the U-Pb ages of the filtered detrital zircon dataset. **(c)** World
120 map, made from Natural Earth @NaturalEarthData.com, showing locations of all samples.

121

122 In Figures 2 and 3 we plot five individual proxies, Ti-in-zircon temperatures, Eu/Eu*, Yb/Gd,
123 Th/Yb, and U/Yb. We plot both average global trends using the weighted bootstrap approach and

124 compare the data with previous publications (plotted using the same method), and we plot
125 individual trends for the four continents with large data coverage (Antarctica, Asia, North
126 America, and Oceania).

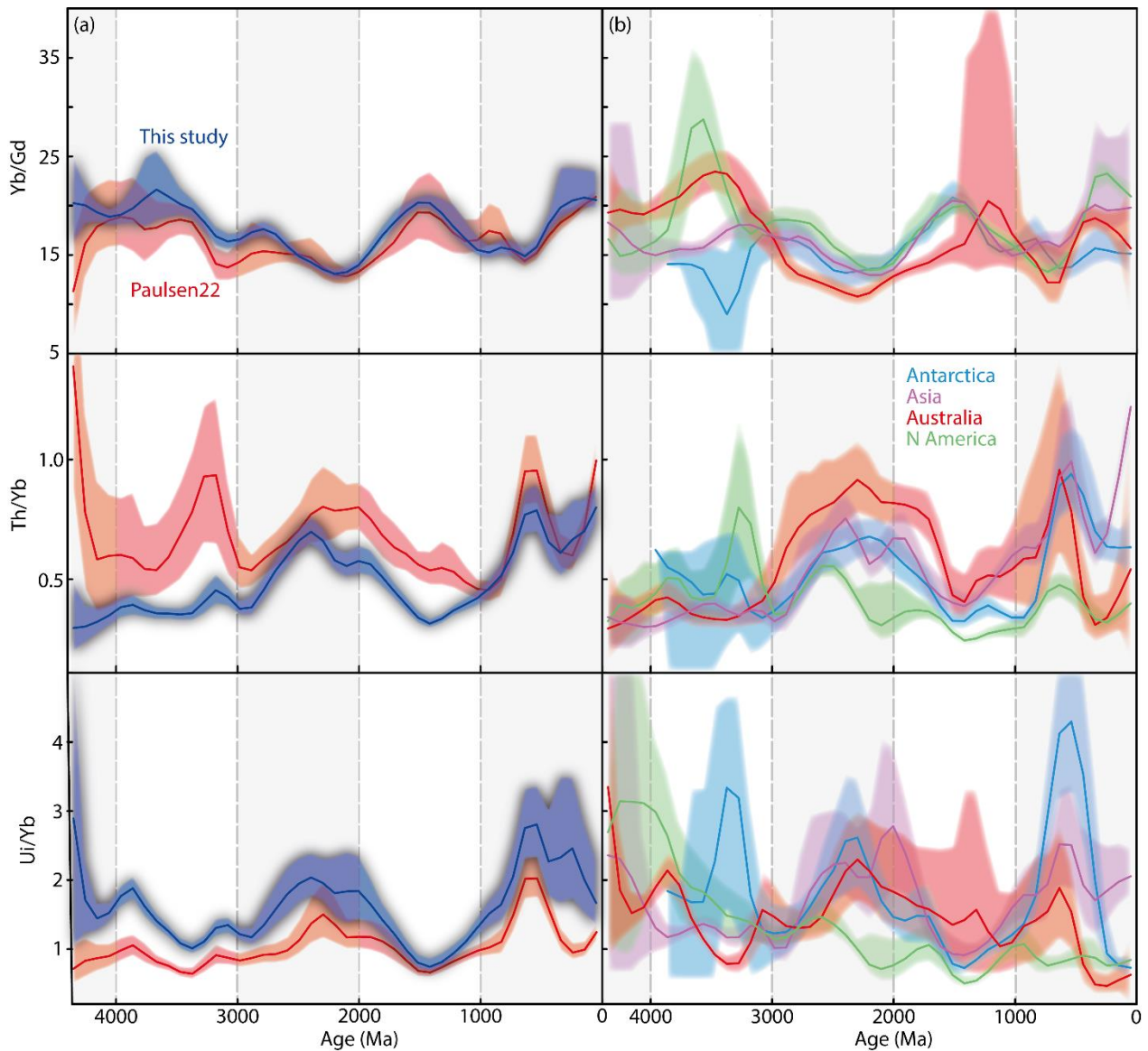
127



128

129 **Figure 2 (a)** Ti-in-zircon temperatures and Eu/Eu* for our global detrital zircon database
130 compared to previous databases (Balica et al., 2020; Tang et al., 2021b). **(b)** Continental-scale
131 comparison of our detrital zircon database comparing trends from four continents. All plots are
132 shown as weighted bootstrap means with error bands representing 2 standard errors of the mean.

133



134

135 **Figure 3 (a)** Yb/Gd, Th/Yb, and U/Yb for our global detrital zircon database compared to a
 136 previous database (Paulsen et al., 2022). **(b)** Continental-scale comparison of our detrital zircon
 137 database comparing trends from four continents. All plots shown as weighted bootstrap means
 138 with error bands representing 2 standard errors of the mean. Note that for our database, U/Yb
 139 incorporates age-corrected U concentrations (U_i/Yb).

140

141 4. Discussion

142 4.1 Robust trends in thermometry?

143 The Ti-based zircon thermometer has long been considered robust, but it is well known that
 144 accurate Si and Ti activities are required to achieve accurate temperature estimates (e.g. Schiller
 145 and Finger, 2019). The pressure dependence of this thermometer has been considered negligible,

146 although recent work implies a subtle pressure effect that needs to be considered for high-
147 pressure zircon growth especially (Crisp et al., 2023). Temperature estimates from single
148 magmatic rocks often exhibit a large range, implying zircon crystallisation over a protracted
149 temperature range (Ickert et al., 2011), and/or diffusion (Bloch et al., 2022). As such, any detrital
150 zircon estimate has to consider that a single temperature datum may relate to a snapshot of a
151 broader magmatic and cooling history. Regarding secular trends in temperatures derived from
152 detrital zircon, these have to be constructed using single choices of Si and Ti activities and
153 pressure and thus may average out some variation that would be exhibited by the true temperature
154 range.

155

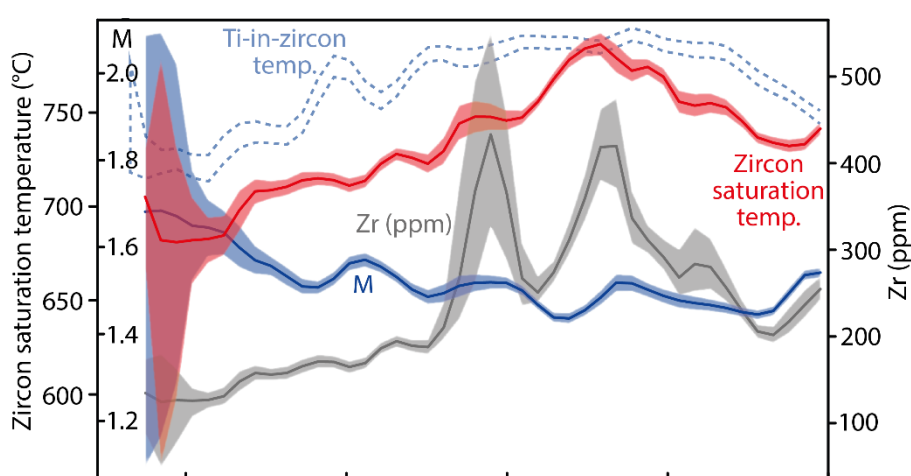
156 Based on a detrital zircon compilation with broad global coverage, Balica et al. (2020) noted “A
157 distinctive increase from 700–800 °C pre-3.2 Ga followed by a gradual decrease since then”.
158 Within our larger dataset, we see a similar increase up to 3.0 Ga, but rather than decreasing, the
159 global trend has a marginal increase up to 1.2 Ga. Only after 1.2 Ga does the trend decrease, and
160 particularly rapidly after 0.7 Ga. Assessing the continent-specific trends, we can see that pre-3.2
161 Ga is varied, with large uncertainties owing to sparse data coverage; however, overall there is a
162 marked increase from values pre- and post- 3 Ga. From 3 to 1 Ga, values for each continent vary,
163 but overall show a broad stability with only minor variation. All continents exhibit lower
164 temperatures in the Phanerozoic, with the onset of decreasing values varying between continents.
165 Based on these observations, the following observations likely represent global processes: 1) an
166 increase in temperatures through the early Archean up to ca. 3 Ga; 2) consistent temperatures (in
167 the range of 750-800 °C) from ca. 3 to 1 Ga; and 3) lower temperatures into the Phanerozoic (ca.
168 750 °C). We note that these absolute values depend on the choice of Si and Ti activities, but the
169 scale of increasing and decreasing temperatures is likely independent of these activities.

170

171 Balica et al. (2020) argued that the apparent change in temperature at ~3.2 Ga “must mark the
172 change from eutectic of the albite-anorthite-quartz system towards progressively higher
173 dehydration melting of biotite and amphibole-bearing rocks”. In contrast, Verdel et al. (2021)
174 simply relate higher zircon temperatures throughout the Proterozoic to higher crustal
175 temperatures. If Ti-in-zircon simply recorded the highest primary temperatures of a magmatic
176 rock, then the secular changes may indeed record changing reactions and/or geotherms. However,
177 zircon temperatures in magmatic rocks relate to multiple petrologic variables, including the
178 timing and temperature of zircon saturation during a magma’s evolution, which in turn is related

179 to magma chemistry. Thus, secular trends in zircon thermometry likely result from multiple
 180 underlying variables that also exhibit secular changes; these include most obviously the changing
 181 geochemistry of igneous rocks (i.e. Keller and Schoene, 2012), but may also include changing
 182 cooling rates. Deconvolving the contributions of different processes that led to the apparent
 183 global secular pattern is not trivial; however, we demonstrate using a global database of
 184 intermediate-felsic igneous rock compositions (Figure 4) that secular changes in magmatic
 185 composition, both the Zr abundance and M (relating to alkali content) likely have a controlling
 186 factor. These variables will change the saturation and growth history of zircon in magmatic rocks,
 187 and thus, in turn, will also be reflected in Ti-based zircon thermometry.

188



189

190 **Figure 4.** Comparison of whole-rock and zircon-based temperatures. The dashed trend is Ti-in-
 191 zircon thermometry from the global detrital zircon database, as in Figure 2. Red, grey and blue
 192 trends are based on the global igneous felsic rock compilation of Gard et al. (2019), and
 193 demonstrate the zircon saturation temperatures calculated using the equation of Boehnke et al.
 194 (2018), Zr abundance (ppm) and M value, respectively. All trends shown as weighted bootstrap
 195 means with error bands representing 2 standard errors of the mean.

196

197 4.2 Eu/Eu^* , a robust 'barometer'?

198 There has been a substantial effort in recent years to use whole-rock geochemical signatures of
 199 igneous rocks to estimate the depth of melting and/or the thickness of the crustal column, a field
 200 that has recently been coined 'chemical mohometry' (Luffi and Ducea, 2022). Many geochemical
 201 signatures rely on the contrasting behaviour between garnet and plagioclase which are stable at
 202 deep and shallow crustal levels, respectively (e.g. Alonso-Perez et al., 2009). Well-constrained
 203 trends between average arc thicknesses and whole-rock La/Yb and Sr/Y have been demonstrated

204 (Chapman et al., 2015; Profeta et al., 2015). Tang et al. (2021a) argued that zircon could be used
205 in the same manner, suggesting that if Eu anomalies reflect plagioclase fractionation, then these
206 could equally be linked to crustal thickness. Their proxy for crustal depth links Eu/Eu^* to whole-
207 rock La/Yb , and relies on previous constraints for thickness from La/Yb . However, problems
208 with this proxy are plentiful: 1) the statistical treatment relies on an indirect correlation through a
209 whole-rock proxy; 2) Eu anomalies are partially controlled by redox; 3) plagioclase and garnet
210 stability in the crust varies with composition, conditions (i.e. water content) and geothermal
211 gradient (Tamblyn et al., 2022; Triantafyllou et al., 2022); and 4) Eu/Eu^* will be imparted from
212 the magma source, with contamination of magmas altering the primary Eu signature (Bell and
213 Kirkpatrick, 2021). As such, Triantafyllou et al. (2022) cautioned against the use of this proxy for
214 understanding crustal thickness in deep time, and we echo those concerns.

215

216 Tang et al. (2021b) investigated Eu anomalies of a global detrital zircon dataset, demonstrating
217 that the greatest negative anomalies – and thus, lower crustal thicknesses, occurred in a period
218 known as Earth’s ‘Middle Age’ (1.8-0.8 Ga). Our average global mean replicates the broad
219 overall trend of decreasing then increasing values between 3 and 0 Ga; however, there is a critical
220 difference that is pertinent to the conclusions of Tang et al. (2021b). Specifically, the minima in
221 that study broadly span the Mesoproterozoic eon (1.6-1.0 Ga), whereas, in our dataset, the
222 minima are offset to younger ages (~1.0 Ga to 0.7 Ga). Examining the continent-based trends in
223 Figure 2, we argue there is even more cause for concern. Although all continents seem to exhibit
224 low values between 1.2 and 0.5 Ga, data before 1.5 Ga are highly varied, with significant
225 variation between the continents throughout the Archean. As such, we question the validity of the
226 averaged global trend as representing global secular change. A direct correlation between low Eu
227 anomalies and Earth’s Middle Age is negated (c.f. Tang et al., 2021b). Furthermore, based on the
228 arguments above, we suggest that a correlation between Eu/Eu^* and crustal thickness is not
229 warranted, and we argue the jury is still out as far as estimates of mid-Proterozoic crustal
230 thickness are concerned.

231

232 *4.3.1 HREE-dependant proxies*

233 Several petrogenetic zircon-based proxies use contrasting behaviour of REEs, such as light to
234 heavy or middle to heavy REE, or involve other elements that are mobile/immobile under certain
235 conditions. Commonly used ratios include Th/Yb , U/Yb , La/Yb , and Yb/Gd . Paulsen et al. (2021,
236 2022) argue that because Th is enriched relative to other elements as the continental crust

237 matures, increasing Th/Yb ratios in zircon can be used as a proxy for evolved magmatism that
238 involves the recycling of older radiogenic crust. U/Yb has variably been used as both a proxy for
239 subduction input and to discriminate continental from oceanic-crust derived zircon (Grimes et al.,
240 2007; Verdel et al., 2021; Paulsen et al., 2021, 2022), owing to the U enrichment from slab-
241 derived fluids during subduction. Yb/Gd is used as a proxy for HREE to MREE enrichment.
242 Since HREE is more compatible with garnet in comparison to most other major igneous minerals,
243 the presence of garnet during zircon crystallisation strongly controls the resulting Yb/Gd ratios.
244 Given the pressure dependence on garnet stability, Yb/Gd has been used as a broad proxy for
245 crustal thickness (Paulsen et al., 2021, 2022). Similarly, Verdel et al. (2021) used Lu/Nd as a
246 proxy for HREE/LREE, with their overall premise of low ratios equalling the involvement of
247 thick continental crust being comparable. La/Yb is used as a proxy for LREE to HREE
248 enrichment and equally is related to crustal thickness due to the effect of garnet \pm amphibole on
249 Yb abundance in zircon (Chapman et al., 2015; Balica et al., 2020).

250

251 The use of the above-mentioned ratios as proxies is hindered by a variety of factors. Specific to
252 U, is the fact that U incorporation in zircon likely has a redox control (Loucks, 2021). Four
253 important factors are more generally relevant to all of these proxies and in fact most elemental
254 ratios in zircon: (1) Co-crystallisation of other mineral phases is not always considered. For
255 example, sequestration of HREE in garnet is argued as a factor strongly influencing all of the
256 aforementioned ratios, yet Th incorporation in monazite or allanite is not considered for Th/Yb.
257 (2) The stability of phases that sequester the elements of interest depends on multiple variables
258 beyond pressure, such as temperature and water content (e.g. Tamblyn et al., 2022; Triantafyllou
259 et al., 2022). (3) An important but typically ignored problem, particularly relevant for ratios
260 involving a HREE (i.e. Yb), is that zircon itself has a markedly high partition coefficient for Yb
261 (\sim 200; Claiborne et al., 2018) – orders of magnitude higher than that of most other igneous
262 minerals. Therefore, as soon as zircon starts to crystallise, HREE in the melt will become
263 depleted, and thus the ratio involving REEs will change through the magmatic history whilst
264 zircon is crystallising/dissolving (Zhong et al., 2021). As such, a detrital zircon ratio will be just a
265 snapshot of this complex evolution. (4) Finally, as mentioned above for Eu/Eu*, contamination
266 and assimilation of magmas during their evolution will influence the melt trace element budget,
267 In summary, any single apparent secular trend may reflect multiple processes, and assuming a
268 control by pressure-dependant mineral phases is likely a gross misinterpretation of the data.

269

270 *4.3.2 HREE-dependant trends*

271 Paulsen et al. (2022) described three peaks in Th/Yb in their global dataset, at 3.2, 2.5-1.9, and
272 0.5 Ga, and a period of lower values throughout Earth's Middle Age. Excluding the 3.2 Ga peak,
273 the averaged global trend of our dataset also records these peaks and troughs. Examining the
274 trends in the continent-specific data, it can be seen that all continents exhibit higher values in the
275 broad period 2.7-1.7 Ga, and again at 0.7-0.5 Ga. Minima vary between the continents but
276 overlap in the broad region of 1.5-0.8 Ga. As noted by Paulsen et al. (2022), these periods of
277 elevated Th/Yb ratios broadly match increases in recycling of older crust as determined by Sr and
278 Hf isotope data. However, we highlight that higher ratios in the late Archean to early
279 Paleoproterozoic overlap in time with the tectono-magmatic lull (Condie et al., 2022), rather than
280 orogenesis associated with Columbia supercontinent formation at 2.0-1.6 Ga. This observation
281 questions a direct link between Th/Yb ratios and orogenesis, beyond the general issues we
282 highlight above with these petrogenetic proxies.

283

284 Paulsen et al. (2022) highlighted that peaks in U/Yb correlated with their peaks in Th/Yb, and we
285 see comparable overlap between Th/Yb and U/Yb in our averaged global mean trends. Using the
286 continent-specific data to examine the importance of these trends, we note that U/Yb is somewhat
287 more variable between continents than Th/Yb. Overall, peaks fall between 2.7 to 1.7 Ga, and 0.7-
288 0.5 Ga (with data >3 Ga being highly variable); however, North America does not match the
289 global average, exhibiting a different periodicity of peaks and troughs. The reason for the
290 mismatch between continents may result from different continent-scale orogens dominating
291 different regions, i.e. the Grenville orogen being extensive in North America, and the Pan-
292 African orogen extending through Africa into Asia (India), Australia, and Antarctica.

293

294 Paulsen et al. (2022) demonstrated a broad inverse relationship between Yb/Gd and their other
295 proxies for crustal thickness/maturity (Th/Yb and U/Yb). In our expanded database, this inverse
296 relationship can be seen on a broad level, but there is some offset between the peaks and troughs.
297 Examining the continent-specific data, we see correlative behaviour between three of the four
298 continents shown, with Antarctica clearly having high variability during the Mesoproterozoic.
299 Trends pre-3 Ga are highly variable. If Yb/Gd truly represents the presence or absence of garnet
300 during zircon crystallisation, then at face value, the trends imply minimal garnet presence at ~1.5
301 Ga and ~0.5-0 Ga, and maximum garnet presence at ~2.5-2.0 Ga, and ~1.0-0.6 Ga. However, an
302 important observation is that these trends are uncorrelated to those defined by Eu anomalies,

303 which Tang et al. (2021a) argue are also dictated by the role of plagioclase versus garnet during
304 crystallisation.

305

306 ***4.4 Implications for secular change***

307 As identified by Sundell and Macdonald (2022) for Hf isotope data of large detrital zircon
308 datasets, the results will be dominated by the influence of large orogens and crust-forming events.
309 Not all orogens are characterized by the same geodynamic configuration or resultant isotopic
310 signatures (Spencer et al., 2013), with accretionary versus collisional orogens having different
311 architectures in terms of crustal recycling, crustal thickness, and geothermal gradients; all these
312 variables will influence zircon trace elements compositions in some way. As such, averaged
313 global trends reflect the average of the active orogenesis through time, and specific orogens may
314 record secular changes in continental evolution at different times in different ways. An example
315 of this is the zircon Eu anomaly, which is clearly highly divergent during the Paleoproterozoic,
316 even though this time period is dominated by the formation of the Columbia supercontinent
317 across all continents examined.

318

319 We have only addressed a subset of the numerous trace element proxies used hitherto. As
320 discussed above, each proxy is controlled by multiple competing variables such as redox, co-
321 crystallising mineral assemblage, initial melt composition, and extent of crystal fractionation.
322 None of which are a single function of the pressure of melting or crystallisation. As such, the use
323 of zircon trace element proxies for determining trends in crustal composition or thickness should
324 be used with great caution, or, should at least only be applied to igneous populations (i.e. Moreira
325 et al., 2023). Given the multiple variables behind these trace element ratios, it is perhaps no
326 surprise that correlations between some of the proxies are poor (see Supplementary Figure S3).

327

328 **5. Conclusions**

329 We present a literature database of ~72000 detrital zircon trace element compositions, which
330 allows comparison between continents, and evaluation of the robustness of average global trends.
331 Whereas some trace elements/ratios are consistent across continents, i.e. Ti-in-zircon
332 temperatures, others are highly variable. In particular, Eu/Eu* is highly variable between
333 different continents, implying that the average global trend does not simply represent secular

334 change in crustal thickness. Moreover, we argue that because zircon trace element ratios result
335 from the interplay of multiple competing petrologic variables, trace element proxies for crustal
336 composition and thickness are fraught with uncertainties and should be heavily caveated.

337

338 **Acknowledgements**

339 The authors would like to thank Oscar Laurent for discussion, Thea Hinks for sharing code, and
340 the reviewers for their comments. NR publishes with the permission of the Director of the British
341 Geological Survey and is partly supported by funding from the UK Natural Environment
342 Research Council (NE/S011587/1).

343

344 **Author Credits**

345 **NR** – conceptualization, data curation, data analysis, writing, reviewing and editing; **SP** – data
346 curation, reviewing and editing; **CS** – data analysis, reviewing and editing; **CBK** – reviewing and
347 editing; **ST** – reviewing and editing.

348

349 **Data availability**

350 Data and methods associated with this paper are stored and accessible from Figshare:

351 <https://figshare.com/s/89d01010d6a7ba4c9592>

352

353 **Funding**

354 No funding was associated with this study.

355

356 The Authors declare no conflict of interest.

357

358

359

360

361 **References**

- 362 1. Alonso-Perez, R., Müntener, O. and Ulmer, P., 2009. Igneous garnet and amphibole
363 fractionation in the roots of island arcs: experimental constraints on andesitic
364 liquids. *Contributions to Mineralogy and Petrology*, 157, 541.
- 365 2. Balica, C., Ducea, M.N., Gehrels, G.E., Kirk, J., Roban, R.D., Luffi, P., Chapman, J.B.,
366 Triantafyllou, A., Guo, J., Stoica, A.M. and Ruiz, J., 2020. A zircon petrochronologic view
367 on granitoids and continental evolution. *Earth and Planetary Science Letters*, 531, 116005.
- 368 3. Bell, E.A. and Kirkpatrick, H.M., 2021. Effects of crustal assimilation and magma mixing on
369 zircon trace element relationships across the Peninsular Ranges Batholith. *Chemical*
370 *Geology*, 586, p.120616.
- 371 4. Bloch, E.M., Jollands, M.C., Tollan, P., Plane, F., Bouvier, A.S., Hervig, R., Berry, A.J.,
372 Zaubitzer, C., Escrig, S., Müntener, O. and Ibañez-Mejia, M., 2022. Diffusion anisotropy of
373 Ti in zircon and implications for Ti-in-zircon thermometry. *Earth and Planetary Science*
374 *Letters*, 578, p.117317.
- 375 5. Brudner, A., Jiang, H., Chu, X. and Tang, M., 2022. Crustal thickness of the Grenville
376 orogen: A Mesoproterozoic Tibet?. *Geology*, 50, 402-406.
- 377 6. Chapman, J.B., Ducea, M.N., DeCelles, P.G. and Profeta, L., 2015. Tracking changes in
378 crustal thickness during orogenic evolution with Sr/Y: An example from the North American
379 Cordillera. *Geology*, 43, 919-922.
- 380 7. Claiborne, L.L., Miller, C.F., Gualda, G.A., Carley, T.L., Covey, A.K., Wooden, J.L. and
381 Fleming, M.A., 2018. Zircon as magma monitor: Robust, temperature-dependent partition
382 coefficients from glass and zircon surface and rim measurements from natural
383 systems. *Microstructural geochronology: planetary records down to atom scale*, pp.1-33.
- 384 8. Condie, K.C., Pisarevsky, S.A., Puetz, S.J., Spencer, C.J., Teixeira, W. and Faleiros, F.M.,
385 2022. A reappraisal of the global tectono-magmatic lull at~ 2.3 Ga. *Precambrian*
386 *Research*, 376, p.106690.
- 387 9. Crisp, L.J., Berry, A.J., Burnham, A.D., Miller, L.A. and Newville, M., 2023. The Ti-in-
388 zircon thermometer revised: The effect of pressure on the Ti site in zircon. *Geochimica et*
389 *Cosmochimica Acta*. doi.org/10.1016/j.gca.2023.04.031
- 390 10. Gard, M., Hasterok, D. and Halpin, J.A., 2019. Global whole-rock geochemical database
391 compilation. *Earth System Science Data*, 11, 1553-1566.
- 392 11. Grimes, C.B., John, B.E., Kelemen, P.B., Mazdab, F.K., Wooden, J.L., Cheadle, M.J.,
393 Hanghøj, K. and Schwartz, J.J., 2007. Trace element chemistry of zircons from oceanic crust:
394 A method for distinguishing detrital zircon provenance. *Geology*, 35, 643-646.

- 395 12. Ickert, R.B., Williams, I.S. and Wyborn, D., 2011. Ti in zircon from the Boggy Plain zoned
396 pluton: implications for zircon petrology and Hadean tectonics. *Contributions to Mineralogy
397 and Petrology*, 162, pp.447-461.
- 398 13. Keller, C.B. and Schoene, B., 2012. Statistical geochemistry reveals disruption in secular
399 lithospheric evolution about 2.5 Gyr ago. *Nature*, 485, 490-493.
- 400 14. Liu, H., McKenzie, N.R., Colleps, C.L., Chen, W., Ying, Y., Stockli, L., Sardud, A. and
401 Stockli, D.F., 2022. Zircon isotope–trace element compositions track Paleozoic–Mesozoic
402 slab dynamics and terrane accretion in Southeast Asia. *Earth and Planetary Science
403 Letters*, 578, 117298.
- 404 15. Loucks, R.R., Fiorentini, M.L. and Henríquez, G.J., 2020. New magmatic oxybarometer
405 using trace elements in zircon. *Journal of Petrology*, 61, p.egaa034.
- 406 16. Luffi, P. and Ducea, M.N., 2022. Chemical mohometry: Assessing crustal thickness of
407 ancient orogens using geochemical and isotopic data. *Reviews of Geophysics*, 60,
408 p.e2021RG000753.
- 409 17. McKenzie, N.R., Smye, A.J., Hegde, V.S. and Stockli, D.F., 2018. Continental growth
410 histories revealed by detrital zircon trace elements: A case study from India. *Geology*, 46,
411 275-278.
- 412 18. Moreira, H., Buzenchi, A., Hawkesworth, C.J. and Dhuime, B., 2023. Plumbing the depths of
413 magma crystallization using $^{176}\text{Lu}/^{177}\text{Hf}$ in zircon as a pressure proxy. *Geology*,
414 doi.org/10.1130/G50659.1
- 415 19. Paulsen, T., Deering, C., Sliwinski, J., Chatterjee, S., Bachmann, O. and Guillong, M., 2021.
416 Crustal thickness, rift-drift and potential links to key global events. *Terra Nova*, 33, 12-20.
- 417 20. Paulsen, T., Deering, C., Sliwinski, J., Chatterjee, S. and Bachmann, O., 2022. Continental
418 magmatism and uplift as the primary driver for first-order oceanic $^{87}\text{Sr}/^{86}\text{Sr}$ variability with
419 implications for global climate and atmospheric oxygenation. *GSA Today*, 32, 4-10.
- 420 21. Profeta, L., Ducea, M.N., Chapman, J.B., Paterson, S.R., Gonzales, S.M.H., Kirsch, M.,
421 Petrescu, L. and DeCelles, P.G., 2015. Quantifying crustal thickness over time in magmatic
422 arcs. *Scientific reports*, 5, 1-7.
- 423 22. Puetz, S.J., Spencer, C.J. and Ganade, C.E., 2021. Analyses from a validated global UPb
424 detrital zircon database: enhanced methods for filtering discordant UPb zircon analyses and
425 optimizing crystallization age estimates. *Earth-Science Reviews*, 220, 103745.
- 426 23. Roberts, N.M.W. and Spencer, C.J., 2015. The zircon archive of continent formation through
427 time. Geological Society of London Special Publication, 389, doi.org/10.1144/SP389.1
- 428 24. Schiller, D. and Finger, F., 2019. Application of Ti-in-zircon thermometry to granite studies:
429 problems and possible solutions. *Contributions to Mineralogy and Petrology*, 174, pp.1-16.

- 430 25. Spencer, C.J., Hawkesworth, C., Cawood, P.A. and Dhuime, B., 2013. Not all
431 supercontinents are created equal: Gondwana-Rodinia case study. *Geology*, *41*, 795-798.
- 432 26. Sundell, K.E. and Macdonald, F.A., 2022. The tectonic context of hafnium isotopes in
433 zircon. *Earth and Planetary Science Letters*, *584*, 117426.
- 434 27. Tamblyn, R., Hasterok, D., Hand, M. and Gard, M., 2022. Mantle heating at ca. 2 Ga by
435 continental insulation: Evidence from granites and eclogites. *Geology*, *50*, 91-95.
- 436 28. Tang, M., Ji, W.Q., Chu, X., Wu, A. and Chen, C., 2021a. Reconstructing crustal thickness
437 evolution from europium anomalies in detrital zircons. *Geology*, *49*, 76-80.
- 438 29. Tang, M., Chu, X., Hao, J. and Shen, B., 2021b. Orogenic quiescence in Earth's middle
439 age. *Science*, *371*, 728-731.
- 440 30. Triantafyllou, A., Ducea, M.N., Jepson, G., Hernández-Montenegro, J.D., Bisch, A. and
441 Ganne, J., 2022. Europium anomalies in detrital zircons record major transitions in Earth
442 geodynamics at 2.5 Ga and 0.9 Ga. *Geology*, doi.org/10.1130/G50720.1
- 443 31. Verdel, C., Campbell, M.J. and Allen, C.M., 2021. Detrital zircon petrochronology of central
444 Australia, and implications for the secular record of zircon trace element
445 composition. *Geosphere*, *17*, 538-560.
- 446 32. Wu, G.H., Chu, X., Tang, M., Li, W. and Chen, F., 2023. Distinct tectono-magmatism on the
447 margins of Rodinia and Gondwana. *Earth and Planetary Science Letters*, *609*, 118099.
- 448 33. Zhong, S., Li, S., Seltnann, R., Lai, Z. and Zhou, J., 2021. The influence of fractionation of
449 REE-enriched minerals on the zircon partition coefficients. *Geoscience Frontiers*, *12*,
450 101094.